Polym. Bull. (2011) 67:1991–2016
DOI 10.1007/s00289-011-0616-7

ORIGINAL PAPER

Nanocomposites of PLA/PP blends based on sepiolite

K. Nuñez · C. Rosales · R. Perera · N. Villarreal · J. M. Pastor

Received: 2 February 2011 / Revised: 7 June 2011 / Accepted: 21 August 2011 /
Published online: 14 September 2011

Abstract In the present study, the effectiveness of four polymers grafted with maleic anhydride used as compatibilizers in blends with poly(lactic acid) and its composites with sepiolite as matrices was evaluated in terms of transmission and scanning electron microscopy, oscillatory shear flow and tensile properties. Two polypropylenes were used as dispersed phases in the blends prepared in a corotating twin-screw extruder. Results showed that the compatibilized blends prepared without clay have higher susceptibility to isothermal degradation and higher tensile toughness than those prepared with sepiolite. The blend with the grafted metallocene polyethylene as compatibilizer exhibited the highest tensile toughness. The composites based on polyblends with polypropylene displayed lower tensile strength and Young's modulus values, increased values of elongation at break, tensile toughness, complex viscosity, and storage modulus compared to those of the nanocomposite of PLA. These results are related to the clay dispersion, to the type of morphology of the different blends, to the grafting degree of the compatibilizers, and to the migration of the sepiolite toward the PP interface.

Keywords Poly(lactic acid) · PP · Tensile toughness · Sepiolite · Nancomposites · Blends

K. Nuñez · C. Rosales · R. Perera
Dpto. de Mecánica, Universidad Simón Bolívar, Apdo 89000, Caracas 1081, Venezuela

K. Nuñez (✉) · R. Perera · J. M. Pastor
Dep. de Física de la Materia Condensada E.I.I, Universidad de Valladolid, Paseo del Cauce 59, 47011 Valladolid, Spain
e-mail: karnun@cidaut.es

N. Villarreal · J. M. Pastor
CIDAUT Foundation for Research and Development in Transport and Energy, Parque Tecnológico de Boecillo, 47151 Valladolid, Spain

Introduction

It is difficult to design low cost materials that meet technical requirements for packaging, such as good mechanical, barrier, and biodegradation properties. Since packaging and containers with high barrier properties are usually made by co-extrusion, nanocomposite technology, and/or polymer blending are beneficial alternatives in designing products with the required properties for these applications [1, 2]. Poly(lactic acid) (PLA) is a biodegradable polymer with very low tensile ductility and poor barrier properties to water, O_2, and CO_2 [3]. On the contrary, polypropylene (PP) is a commodity low-cost polymer with high tensile ductility and good barrier properties to water. Hence, a material obtained blending a nanocomposite of PLA with PP could be an alternative to meet the desired requirements for different packaging applications, though immiscibility will result.

In immiscible polymer blends the morphology achieved depends, in general, on the blend composition, interfacial tension between the components, viscosity ratio, melt elasticity of the components, and processing history. It is now well established that the phase morphology of immiscible polymer blends without clays can be controlled by addition of compatibilizers, which can act as interfacial agents [4, 5]. PLA has been combined, for example, with other thermoplastics (PP, PA-6, PE, etc.) in order to improve its toughness [6–8]. On the other hand, most of the literature regarding PLA nanocomposites is devoted to lamellar layered silicates [1, 9–11]. Although there are few studies about polymer nanocomposites based in sepiolite, a high level of reinforcement was found in these nanocomposites [12, 13]. In addition, material parameters that can be controlled and which can have a profound influence on the nature and properties of the final nanocomposite blends include the type of clay, the choice of clay pre-treatment, the selection of the blend components, and the way in which the polymers are incorporated into the nanocomposite. Since clay nanocomposites can produce dramatic improvements in a variety of properties, it is important to understand the factors affecting the dispersion degree of the clay [1, 2]. Some immiscible blends of clay nanocomposites show lower dispersed particle sizes than similar blends without the nanofiller and compatibilizer agents.

Among the different mechanisms of compatibilization in those blends, the migration of the clay toward the blend interface where a solid barrier is formed that inhibits or prevents the coalescence of the dispersed polymer drops and/or the high viscosity of the nanocomposites that reduces the particle sizes are noteworthy [14]. Although nanocomposites of PLA with montmorillonite and sepiolite have been studied [13], the factors that influence or determine the sepiolite dispersion in blends of PLA with polyolefins have been less investigated. Therefore, the main goal of this article is to study the effectiveness of four polymers grafted with maleic anhydride (MA): a styrene/ethylene-butylene/styrene rubber, two PPs, and a metallocene polyethylene (PEm) as tensile toughening materials in nanocomposite blends with sepiolite, PLA as the matrix phase and polypropylene as the polymeric dispersed phase. The resultant materials were evaluated in terms of SEM and TEM morphology, and rheological and tensile properties determinations. Blends without clay were also evaluated for comparison purposes. The isothermal degradation of the materials was studied as well by dynamic rheometry at 200 °C.

Experimental

Materials

A poly(lactic acid) and two polypropylenes with different weight-average molecular weights (PP1 and PP2) were used as the continuous and dispersed phases in the blends, respectively. Four polymers functionalized with maleic anhydride (MA) were used as compatibilizing agents. Two of them were commercial grades: a styrene/ethylene-butylene/styrene rubber (SEBS-g-MA) from Shell Chemical (Kraton FG-1901) and a grafted polypropylene (PP3-g-MA). The remaining two were functionalized by us in our laboratory: the same polypropylene (PP1) used as dispersed phase and a metallocene polyethylene (PEm). In the PP1 and PEm grafting, maleic anhydride (MA, Riedel-de Haën) and dicumyl peroxide (DCP, Aldrich Chemical Company) were employed as the functionalization monomer and initiator, respectively, both used as received. The clay used for the preparation of the PLA nanocomposite blends was a commercial sepiolite with a fibrilar particle shape (Pangel HV CDT-11) supplied by Tolsa. S.A. (Spain). The dimensions of a single sepiolite fiber vary between 0.2 and 3 μm in length, 10–30 nm in width, and 5–10 nm in thickness, with an average aspect ratio of about 27 and a very high surface area (300 m^2/g) [15]. The sepiolite was not modified. The characteristics of the neat polymers employed are shown in Table 1.

Functionalization of the PP in the internal mixer

To perform the functionalization of the PP1 and the PEm, an internal mixer or Rheomix made by Haake was employed. The reaction was carried out at 200 °C, in batches of 50 g (an 80% of the mixer capacity). The frequency of the rotors was set at 60 rpm, and the polymer was melted and mixed during 2 min. At that moment, the monomer (4 phr) was added and mixed for two more minutes at the same frequency. Then, the initiator was fed into the equipment and mixed for three additional minutes. Finally, the grafted product was discharged.

Table 1 Characteristics of the neat materials

Material	Commercial name*	Supplier	$M_w \times 10^{-5}$ (g/mol)	MFI[a] (dg/min)
PLA	PLA2002D Natureworks	Cargill-Dow	2.10[b]	5
PP1	PPJ300	Propilven	5.6[c]	1.4
PP2	Moplen HP501L	Layondell Basell	3.9[c]	6.0
PEm	Engage 8411	Du Pont-Dow	0.55[a]	18
PP3-g-MA	Polybond 3200	Chemtura	–	115

Weight-average molecular weight (M_w) and melt flow index (MFI)

[a] Reported by suppliers, [b] given by Signori et al. [16], and [c] determined by the Newtonian viscosity at 180 °C [17, 18]

Preparation of the PLA composites (nPLA) and blends

The PLA composites and blends were prepared in a Berstorff (ECS-2E25) corotating intermeshing twin-screw extruder at 200 °C (die temperature) and 100 rpm. In the PLA composite preparation, all the blend components were fed through the first port of the extruder and the sepiolite through the second port. The solid materials were starved fed to the extruder by a solid feeder and the extrudates were cooled in a water bath and pelletized afterward. The test specimens for determining the properties were compression molded for 2.5 min at 200 °C. The PLA and its composites and blends without sepiolite were dried in a vacuum oven at 50 °C for 24 h before mixing and testing. The sepiolite clay was also dried before mixing at 100 °C for 4 h. Six PLA composites with sepiolite clay were prepared. Three of them were made with the polypropylene with the higher molecular weight (PP1) as dispersed phase and different compatibilizer agents (SEBS-g-MA and PP1-g-MA). In the other three composites, PP2 was employed as dispersed phase, and PP1-g-MA, PP3-g-MA, and a PEm-g-MA were used as compatibilizer agents. Therefore, six blends without sepiolite clay were also prepared for comparison purposes. Two proportions of the dispersed phases were also used in the PLA blends without sepiolite and in the PLA composites. The proportions and/or the compositions of the blends and composites are shown in Table 2.

Characterization

The polyolefins grafted in our laboratory were analyzed by FTIR spectroscopy in order to determine the degree of maleic anhydride grafted onto them (grafting degree). Ungrafted monomer remaining from (or after) the reaction was removed by dissolving the grafted polyolefins in *o*-dichlorobenzene, followed by precipitation with acetone and by vacuum filtration. The final products (PP1-g-MA and PEm-g-MA) were vacuum dried at 70 °C for 48 h. Thin films were then obtained by compression molding at 200 °C and their FTIR spectra were recorded employing a Bruker FTIR-ATR Vertex 70 spectrometer, in the 4000–400 cm^{-1} wavelength range with a nominal resolution of 4 cm^{-1}. The methodologies established by Nachtigall et al. [19] for grafted polypropylenes and that reported by Moad [20] for functionalized polyethylenes were employed to determine the grafting degree of the commercially available grafted PP (PP3-g-MA) and both polyolefins grafted by us. The melting and crystallization behaviors of the neat polymers were determined by Differential Scanning Calorimetry (DSC) using a Mettler Toledo DCS 821/400. 10 mg of the samples were heated to 280 °C, held for 5 min at this temperature, then cooled to −20 °C and heated again to 280 °C, at constant rates of 10 °C/min and under constant nitrogen flow. In all cases, second heating scans were used for analysis**.** The heats of crystallization for 100% crystalline materials were taken as 93, 293, and 207 J/g for PLA, PE, and iPP, respectively [21–23].

In addition, the neat polymers were subjected to oscillatory shear in a Haake RS-600 Rheometer over a frequency range of 1–100 rad/s at 200 °C. Isothermal time scans were also performed for up to 30 min at a fixed strain, at a temperature of 200 °C and frequencies of 3.14 and 6.28 rad/s for the neat PLA and 0.5 rad/s for the

Table 2 Blends or composites prepared

Blend	Composition (PLA wt%)	Type of PP (wt%)	Compatibilizer agent and concentration (wt%)	Effective content of sepiolite (wt%)[a]
PLAPP1 1	80	PP1 (17)	PP1-g-AM (3)	–
PLAPP1 2	60	PP1 (34)	PP1-g-AM (6)	
PLAPP1 S	80	PP1 (17)	SEBS-g-MA (3)	–
PLAPP2 A	80	PP2 (17)	PP3-g-AM (3)	–
PLAPP2 B	80	PP2 (17)	PEm-g-MA (3)	–
PLAPP2 C	80	PP2 (17)	PP1-g-AM (3)	–
nPLA	95	–	–	4.5
nPLAPP1 1	75	PP1 (17)	PP1-g-AM (3)	6.2
nPLAPP1 2	55	PP1 (34)	PP1-g-AM (6)	6.2
nPLAPP1 S	75	PP1 (17)	SEBS-g-MA (3)	5.0
nPLAPP2 A	75	PP2 (17)	PP3-g-AM (3)	4.1
nPLAPP2 B	75	PP2 (17)	PEm-g-MA (3)	3.9
nPLAPP2 C	75	PP2 (17)	PP1-g-AM (3)	3.6

[a] Determined by means of TGA at 600 °C

PLA, PLA nanocomposite (nPLA) and its blends and composites because of the thermo-oxidative degradation of the PLA with time at high temperatures. In order to analyze the morphology of the obtained materials, samples of the PLA composite and its blends were observed through Transmission Electron Microscopy (TEM), using a JEOL JEM 2000FX Electron Microscope, with an acceleration voltage of 200 kV. The specimens were prepared by ultramicrotomy (Ultracut S from Leica). Furthermore, the blend without clay prepared with PP1 as dispersed phase and SEBS-g-MA as compatibilizer agent (PLAPP1 S) was stained with osmium tetroxide (OsO_4). On the other hand, the surface of cryogenically fractured specimens was observed by Scanning Electron Microscopy (SEM) in a Hitachi S-4700 Electron Microscope with 20 kV of accelerating voltage, after gold coating.

Tensile properties

The tensile tests were performed using a Lloyd instrument at a crosshead speed of 1 mm/min at room temperature according to ASTM D-638 Standard Procedure. The PLA and its nanocomposites and blends were dried in a vacuum oven at 50 °C for 24 h before testing.

Results and discussion

The main objective of this work was to study the effectiveness of four polymers grafted with maleic anhydride (MA) as tensile toughening materials in nanocomposite blends with sepiolite, PLA as the matrix phase and polypropylene as the

polymeric dispersed phase. To do so, it is important to bear in mind that the tensile properties of the PLA blends and composites are affected by their morphology, which is developed during blending. The process of blending involves the stretching of drop-like particles until fibers are formed, followed by the rupture of these filaments in order to form smaller drops. The coalescence of these drops would, in turn, create larger ones. The balance of these processes determines the final particle size which is controlled by the viscosity of the components (the viscosity ratio), the melt elasticity, shear stresses and rates in the matrix, the mobility of the interphase, and the surface tension, since a lower tension promotes the stretching of even smaller drops producing a very fine morphology. This lower tension is the result of the chemical reactions forming the interfacial copolymers. Owing to the presence of these copolymers, the coalescence rate decreases, since they immobilize the interphase, reducing the final particle size in immiscible polymer blends. The use of compatibilizer agents reduces the interfacial tension and improves the adhesion in polyblends without clay, affecting their final properties [4, 5].

In consequence, the grafting degree and viscosities of the functionalized materials, rheological behavior of the matrix and dispersed phase, and degradation and thermal properties of the blend components have to be determined. Moreover, material parameters that should be controlled in composite materials, include the type of filler and proportion, the choice of filler pre-treatment, the selection of the blend components, and the way in which the polymers are incorporated into the composite [4, 5]. In this study, a sepiolite clay was used as filler. On the other hand, nanoparticles can be defined as particles having (one or more) dimensions below 100 nm [1, 2, 10, 11]; in consequence, single fibers of sepiolite could be considered as nanoparticles. In addition, nanomaterials can be defined as materials having structured components with at least one dimension of less than 100 nm. If high dispersion of the sepiolite clay is obtained in the PLA and their blends, these materials could be considered nanocomposites. In several works [12, 13, 24, 25], the neat polymers with sepiolite were considered to be a nanocomposite because of the excellent distribution of the unmodified inorganic filler in its finest elemental units, even at concentrations as high as 5 wt%, with no indication of particle aggregations.

Grafting degree and rheological behavior of the compatibilizer agents

In order to study the influence of the phase interactions between the blend components, the grafting degree and the rheological behavior of the compatibilizer agents were determined. The grafting degrees of the commercial SEBS-g-MA and those of the three grafted polyolefins (PP1-g-MA, PP3-g-MA, and PEm-g-MA) are shown in Table 3. The polyolefins grafted by us (PP1-g-MA and PEm-g-MA) and the commercially available functionalized polypropylene (PP3-g-MA) have similar grafting degrees, while the SEBS-g-MA has the highest. Table 3 also shows the complex viscosity (η^*) and storage modulus (G') at 10 rad/s of frequency for the grafted materials and for the neat PP1, PEm, and SEBS. The PP1-g-MA and SEBS-g-MA samples have lower viscosities and storage modulus values than their neat PP1 and SEBS counterparts. The complex viscosity (η^*) as a function of frequency

Table 3 Grafting degree, complex viscosity (η^*) and storage modulus (G') at 200 °C and 10 rad/s of frequency, Young's modulus (E) and tensile strength (σ_b) of the neat and grafted materials

Material	Grafting degree (wt%)	η^* at $\omega = 10$ rad/s (Pa s)	G' at $\omega = 10$ rad/s (Pa)	E (Pa)	σ_b (Pa)
PP1	–	2915	10120	1450	25
PP1-g-MA	1.01 ± 0.02	420	1040	1450	23
PP3-g-MA	0.88 ± 0.02 (1.0[a])	24	–	1500	30
PEm	–	260	140	22	6.5
PEm-g-MA	0.82 ± 0.05	540	2280	22	6.5
SEBS	–	6147	40133	137	23
SEBS-g-MA	1.6[a]	4615	22926	114	17

[a] Reported by suppliers

and the storage modulus (G') as a function of loss modulus (G'') are also presented in Fig. 1 for the neat and grafted materials.

The rheological behavior of the grafted materials is a consequence of side reactions that also take place during the functionalization reactions (chain β–scissions, chain branching formation or chain extension). The PP1-g-MA has lower viscosity and storage modulus values than its neat PP1 counterpart at constant frequencies. This indicates a drastic reduction of the weight-average molecular weights when the PP1 and SEBS are grafted with MA (see Table 3). These reductions are a consequence of chain β–scissions on the PP1 and SEBS that took place during the grafting reaction [19, 26]. On the contrary, an increase in viscosity and storage modulus was obtained for the PEm-g-MA, when this grafted polyolefin is compared with its neat material (PEm), due to the formation of long chain branches during the functionalization reactions [20] (see Fig. 1b; Table 3). The commercial grafted PP (PP3-g-MA) has a very low value of the storage modulus at 10 rad/s of frequency; hence, it could not be measured at frequencies below that value.

Isothermal degradation

In order to determine the rheological behavior for the PLA, its composites and blends without the influence of degradation effects in the measurements, isothermal time scans were performed in oscillatory shear flow at 200 °C and constant frequencies. According to the model of thermal degradation in a random chain scission mechanism for PDLLA presented by Liu et al. [27], the influence of time in the PDLLA molecular weight can be described according to the following expression:

$$M(0)/M(t) - 1 = M_o K_x t / W \quad (1)$$

where W is the molecular weight of the polymer repeating unit, K_x is the thermal degradation rate constant, and $M(0)$ and $M(t)$ are the molecular weights of the PDLLA at zero time and t, respectively. On the other hand, the influence of the

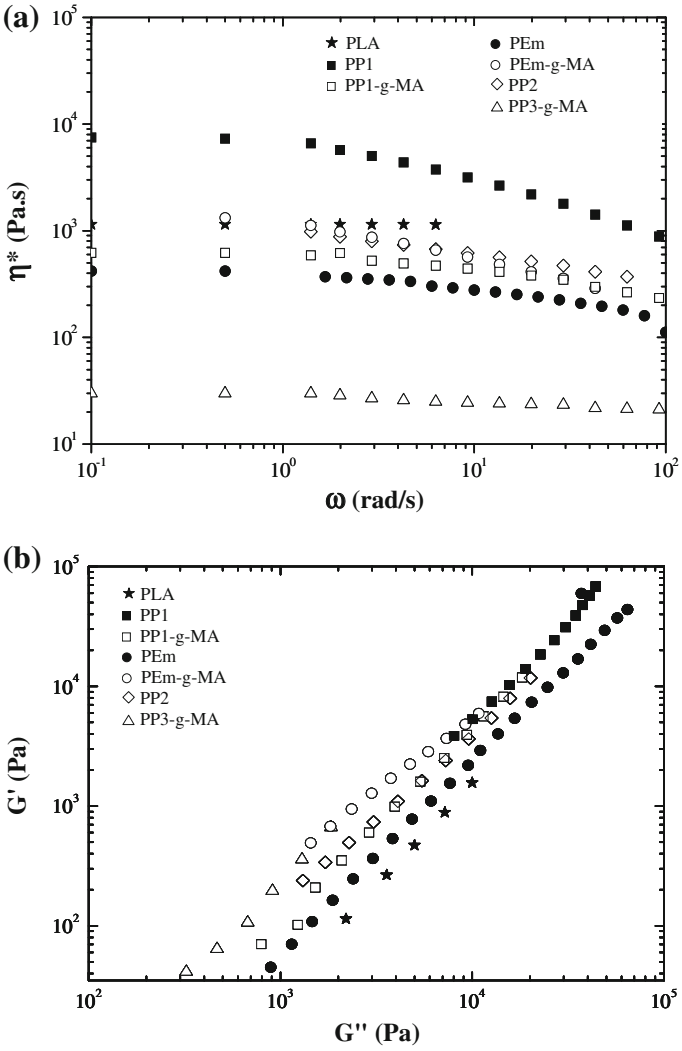

Fig. 1 **a** Complex viscosity (η^*) as a function of frequency, and **b** storage modulus (G') as a function of loss modulus (G'') of the blend components at 200 °C

weight-average molecular weight (M_w) in the Newtonian viscosity (η_0) for linear homopolymer is well known [17]:

$$\eta_0 = A\, M_w^b \tag{2}$$

where A and b are constants at isothermal conditions, and the value of b is about 3.4–3.5. Combining Eqs. 1 and 2, the complex viscosity ($\eta^*(t)$), at time t can be expressed as a function of time:

$$(\eta^*(t))^{-1/b} = (\eta^*(0))^{-1/b} + M_o K_x (\eta^*(0))^{-1/b} t/W \tag{3}$$

To study the degradation using these equations, isothermal time scans were performed in oscillatory shear flow for up to 30 min at a fixed strain, at a temperature of 200 °C, and frequencies of 3.14 and 6.28 rad/s. The good linearity (regression coefficient of 0.997) of the $(\eta^*(t))^{-1/b}$ versus time curves at short time values (before 150 s) for the PLA at 3.14 rad/s of frequency (Fig. 2a) shows that the kinetics of the PLA isothermal degradation reactions was mainly a random chain splitting process and the complex viscosity at zero time ($\eta^*(0)$) can be determined by the intercept of this linear relationship. In a similar way, the viscosity value at 200 °C, 6.28 rad/s of frequency and zero time was calculated. These values and storage modulus at zero time ($G'(0)$) at both frequencies are shown in Table 4. The storage modulus ($G'(t)$) versus the loss modulus ($G''(t)$) curves (at different times) are presented in Fig. 2b. Similar G' versus G'' curves were obtained at both frequencies because the relationship between G' and G'' does not depend on the weight-average molecular weights in linear homopolymers [12].

On the other hand, the influence of time in the complex viscosity curves of neat PLA and its blends without clay and the PLA nanocomposite (nPLA) at a frequency of 0.5 rad/s can be observed in Fig. 3. In order to calculate the loss modulus ($G'(0)$) and the complex viscosity ($\eta^*(0)$) at zero time and 0.5 rad/s of frequency for the PLA and its blends without clay after processing, the data obtained between the time limits of 0–30 min were fitted to high order polynomial equations. The storage modulus at zero time ($G'(0)$) was calculated by the following expression at 0.5 rad/s of frequency:

$$\eta^*(0) = \left(\left(G''^2(0) + G'^2(0)\right)^{0.5}\right)/0.5 \tag{4}$$

High regression coefficients (0.99) were obtained in these high order polynomial expressions with a reduction in the loss modulus (G''), in the storage modulus (G'), and in the complex viscosity (η^*) with time for the PLA and its blends without clay where the dynamic rheological parameters found at zero time are shown in Table 4. The viscosity values of the PLA obtained by the thermal degradation model and that for the high order polynomial equations at 3.14 and 6.28 rad/s of frequencies are very similar. The dynamic rheological parameters at 0.5 rad/s of frequency for the PLA nanocomposite and PLA composites are also presented in Table 4. To obtain the viscosity and storage modulus values at 0.5 rad/s of frequency for these PLA composites, an average of the values at each time was calculated in the evaluated range of time where thermal-stability in the rheometer was found (about 7 min). In addition, polypropylenes (PP1 and PP2) showed a high thermal stability at 0.5 rad/s of frequency and 200 °C in the evaluated time range.

A reduction of the viscosity and storage modulus values with time was found for the neat PLA and PLA blends without sepiolite because of the thermo-oxidative degradation of the neat PLA and PLA matrices of the blends in the dynamic rheometer at 200 °C. However, a lower variation of the viscosity with time was found for the PLA blends than that of neat PLA due probably to the presence of the PPs phases with a higher thermal stability. The complex viscosity and storage modulus values at zero time and 0.5 rad/s of frequency of the blends without clay (PLAPP1 1, PLAPP1 S, and PLAPP2 C) must be related to their morphology and/or

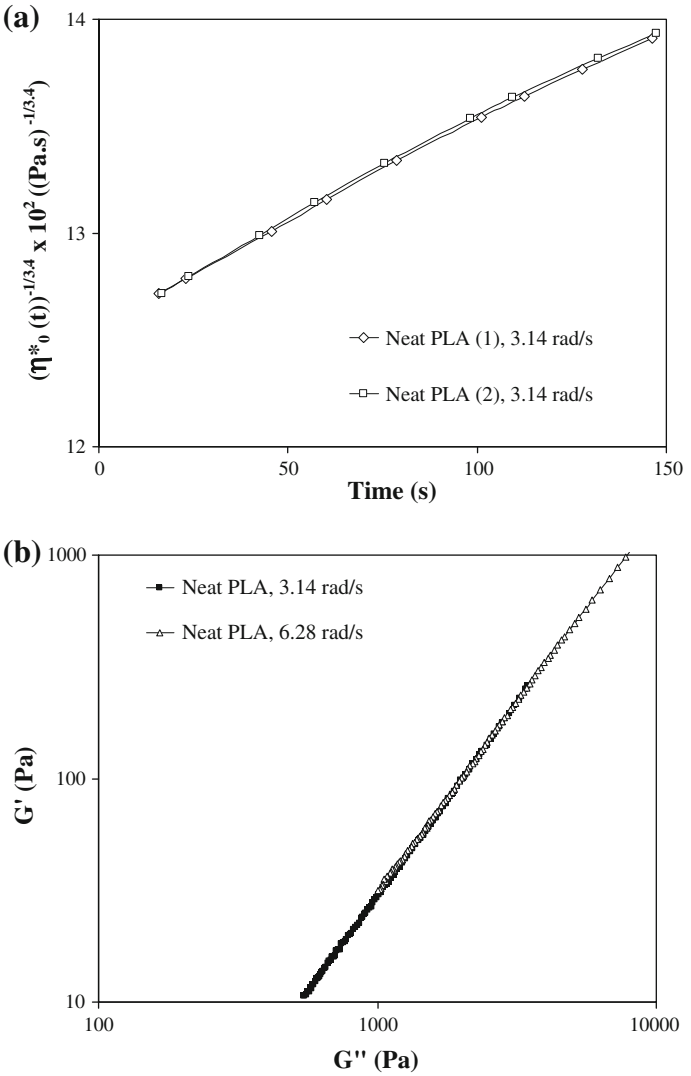

Fig. 2 **a** $(\eta^*(t))^{-1/3.4}$ as a function of time at 3.14 rad/s and 200 °C for samples (*1*) and (*2*), and **b** storage modulus (G') as a function of loss modulus (G'') at different times of the neat PLA at 200 °C and 3.14 and 6.28 rad/s of frequencies

the degradation of their corresponding PLA matrices during their processing. The influence of the blend morphology on the rheological properties of the PLA blends and composites at zero time (without the influence of the thermo-oxidative degradation in the measurements) and at a constant frequency will be presented at the end of the section of tensile properties and rheological behavior of the PLA blends and composites, because of the influence of the blend morphology and interactions between the phases in these results.

Table 4 Dynamic rheological parameters at zero time and 200 °C

Material	$G'(0)$ (Pa)	$G''(0)$ (Pa)	$\eta^*(0)$ (Pa s)	$\eta^*(0)$ (Pa s) from thermal degradation model
PLA at 3.14 rad/s	263	3592	1147	1148
PLA at 6.28 rad/s	870	7178	1151	1140
PLAPP1 1 at 0.5 rad/s	84	362	743	–
PLAPP1 2 at 0.5 rad/s	50	359	725	–
PLAPP1 S at 0.5 rad/s	17	72	148	–
PLAPP2 A at 0.5 rad/s	127	570	1161	–
PLAPP2 C at 0.5 rad/s	111	571	1170	–
nPLA at 0.5 rad/s	124 ± 17	798 ± 45	1615 ± 95	–
nPLAPP1 1 at 0.5 rad/s	340	895	1915	–
nPLAPP1 2 at 0.5 rad/s	1615 ± 114	2355 ± 108	5712 ± 105	–
nPLAPP1 S at 0.5 rad/s	1375 ± 86	1076 ± 174	3492 ± 102	–
nPLAPP2 C at 0.5 rad/s	2474 ± 205	3566 ± 202	8680 ± 202	–
PP1 at 0.5 rad/s	998 ± 25	3162 ± 10	6632 ± 16	–
PP2 at 0.5 rad/s	163 ± 15	798 ± 25	1987 ± 23	–

Storage modulus ($G'(0)$), loss modulus ($G''(0)$), and complex viscosity ($\eta^*(0)$)

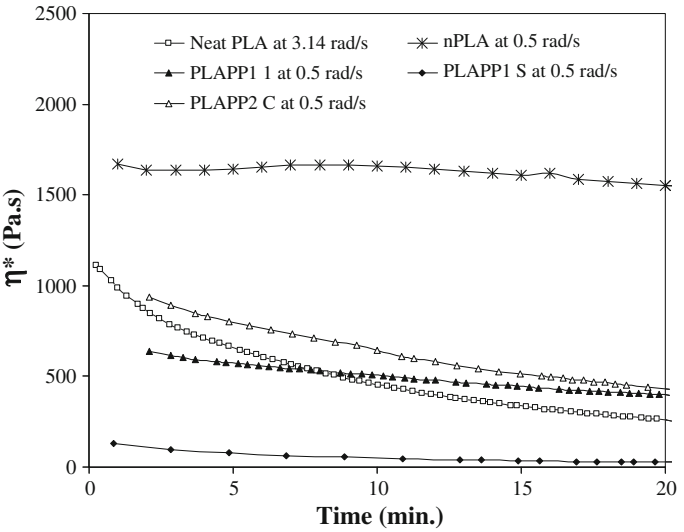

Fig. 3 Complex viscosity (η^*) as a function of time of the neat PLA, PLA nanocomposite (nPLA) and blends without sepiolite (PLAPP1 S, PLAPP1 1, and PLAPP2 C) at 200 °C

No substantial changes in the complex viscosity with time for the PLA nanocomposite (nPLA), and nPLAPP1 S, nPLAPP1 2, and nPLAPP2 C composites were obtained before 7 min. This increase in the thermo-oxidative stability of the composites at 200 °C and times lower than 7 min could be attributed to the physical

barrier to O_2 by the well dispersed sepiolite in these materials, as it will be seen later, and to the interactions between the hydroxy groups of the sepiolite clay and the carbonyl groups of PLA in the PLA nanocomposite (nPLA) or the carbonyl groups of the different compatibilizer agents employed in the blends preparation that provided a barrier effect to the PLA reactive groups in its thermal degradation. Zhou and Xanthos [28] obtained that the PLA degraded 41.2% (determined by viscosity molecular weight) on melt processing compared to the neat PLA. However, the addition of MMT-Na+ or the organomodified layered clay limited this degradation to only 22.1 or 19.6%, respectively. The viscosity ratios of the blend components (η_{PP1}/η_{PLA}, and (η_{PP2}/η_{PLA}) at 200 °C and 3.14 rad/s of frequency as a function of time are presented in Fig. 4. An increase of these viscosity ratios with time was obtained due to the low thermal stability of PLA under thermo-oxidative degradation in a dynamic rheometer at 200 °C and low frequencies. The higher viscosity ratio of the blend components with PP1 are due to the higher viscosities of the PP1 than those of PP2 (see Fig. 1a). The complex viscosity (η^*) as a function of frequency and the storage modulus (G') as a function of the loss modulus (G'') of the neat materials at 200 °C are presented in Fig. 1 for the blend components.

The viscosities of the neat PP1 and its grafted sample (PP1-g-MA), PP2, metallocene polyethylene (PEm) and its grafted material (PEm-g-MA) decreased as the frequency increased, indicating a pseudoplastic behavior (Fig. 1a). Neat PLA shows a characteristic homopolymer-like terminal flow behavior, expressed by the Newtonian behavior and the power law $G' \propto G''^2$ (i.e., terminal zone slope is about 2) at 200 °C. Similar results were obtained by Kim et al. [17]. The complex viscosities at 200 °C presented in Table 4 for the neat PLA without thermo-mechanical degradation are practically the same at 3.14 and 6.28 rad/s of

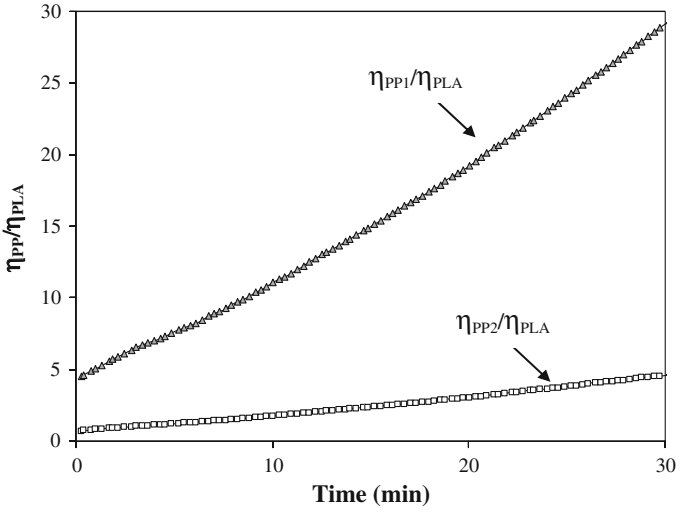

Fig. 4 Viscosities ratios of the blend components (η_{PP1}/η_{PLA} and η_{PP2}/η_{PLA}) as a function of time at 200 °C and 3.14 rad/s of frequency

frequencies. The low shear thinning characters, viscosities and storage moduli, and the high melt flow index of the neat metallocene polyethylene (PEm) are in agreement with its low molecular characteristics (weight-average molecular weight and molecular weight distribution). Owing to its highest weight-average molecular weight and lowest melt flow indexes values (MFI), the neat PP1 sample is more viscous with a higher shear thinning character than its grafted counterpart and the PP2 neat material [17, 26]. The relationship between G' and G'' does not depend on the molecular weight, temperature, and blend composition (in homopolymers with narrow molecular weight distribution and in miscible blends). On the contrary, this plot is very sensitive to the polymer molecular weight distribution in iPP and to the presence of long-chain branching in polyethylenes [17]. Hence, the similar G' versus G'' curves obtained for both neat polypropylenes (PP1 and PP2) and the grafted PP1 (PP1-g-MA). The higher storage modulus of PEm-g-MA (Fig. 1b) than that of neat PEm, at constant loss modulus could be attributed to the presence of long-chain branching content in the former.

On the other hand, the thermal properties of the blend components: glass transition temperature, melting peak temperature, melting enthalpy, and crystallinity degree are reported in Table 5. Neat PLA has a very low melting enthalpy and crystallinity degree because of its rigid backbone and the presence of sepiolite does not affect the glass transition temperature (T_g) of the PLA matrix, which occurs at approximately 64 °C. A weak crystallization exotherm was detected followed by a melting endotherm also at 153 °C in the heating scan, as well as an increase in the melting enthalpy (11.9 J/g) when sepiolite was added to PLA. We assume that the high dispersion of sepiolite increased the nucleation density for the crystallization of PLA as has been previously reported by Fukushima et al. [13]. Similar results were obtained by Tartaglione et al. [25] in their nanocomposites of polypropylene (PP) and poly (butylene terephthalate) (PBT) with sepiolite. Nonetheless, little influence on the crystallinity degree of polyamide-6 nanocomposites with sepiolite was found by Xie et al. [12] and Bilotti et al. [29]. The broad melting range for the neat metallocene polyethylene (PEm) in the second heating scan is a consequence of its high comonomer content (1-octene). In some cases, the melting range for copolymers with a very high comonomer content extends to very low temperatures (in the range of −20 to −40 °C) and almost overlaps the glass transition

Table 5 Thermal properties of the blend components

Material	$T_g \pm 2$ (°C)	$T_m \pm 2$ (°C)	ΔH_m (J/g)	C (%)	ΔT (°C)
PLA	64	153	1.7	–	145–170
nPLA	64	155	11.9	–	145–170
PEm	–	78	76	27	−15–90
PP1	–	169	94	48	80–190
PP2	–	167	96	49	80–190
PP3-g-MA	–	165	99	51	80–180

Glass transition temperature (T_g), melting peak temperature (T_m), melting enthalpy (ΔH_m), crystallinity degree (C), and melting temperature range ΔT

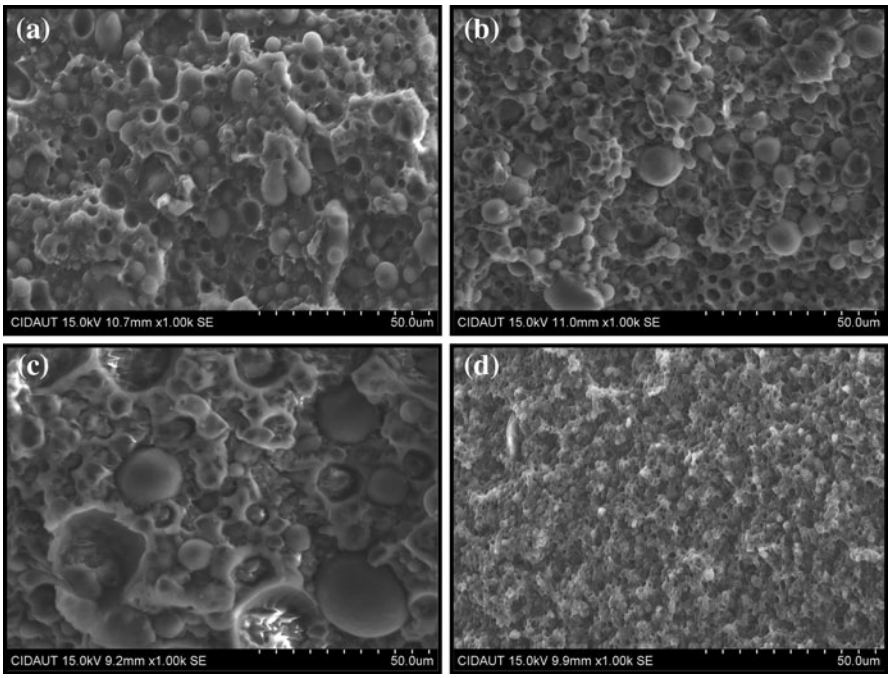

Fig. 5 SEM micrographs of the PLA composites. **a** nPLAPP1 1, **b** nPLAPP2 A, **c** nPLAPP2 B, and **d** nPLAPP2 C

temperature. The low melting enthalpy indicates that the PEm have also very low degrees of crystallinity due to the high level of short-chain branching (SCB) [23]. Finally, the neat polypropylenes display sharper melting and crystallization peaks, characteristics of these polymers [22].

Morphology of the blends and composites by SEM and TEM

Figure 5 depicts the morphology of the PLA composites whose dispersed phases are PP1 and PP2. The number-average-diameter (D_n) of the dispersed phase particles, the ratio between the weight-average and the number-average particle diameters (D_w/D_n) of all studied blends are presented in Table 6. Although four grafted polymers (PP1-g-MA, PP3-g-MA, PEm-g-MA, and SEBS-g-MA) were used as compatibilizer agents in these blends and composites, no morphological evidence of good adhesion between the matrix and the dispersed phases can be seen. During the cryogenically fracture process employed in the surface preparation for SEM characterization, many domains have been pulled away from their previous positions and they remain as empty holes and the particle sizes of the dispersed phases obtained in the blends and composites were very large. Nevertheless, some evidence of interactions between the phases is found in these blends due to their higher tensile toughness than that of neat PLA, as it will be presented later.

Table 6 Number-average diameter (D_n), ratio of weight-average to number-average diameters (D_w/D_n), and tensile properties

Material	D_n (μm)	D_w/D_n	E (MPa)	$\sigma_y \pm 4$ (MPa)	ε_b (%)	$\sigma_b \pm 3$ (MPa)	EF (MJ/m^3)
PLA	–	–	2893 ± 46	–	2.2 ± 0.5	41	0.48 ± 0.05
PP1	–	–	1450 ± 95	25	–	–	–
PP2	–	–	1500 ± 124	34	–	–	–
PLAPP1 1	9.6	1.1	2290 ± 15	25	30 ± 2	17	6.2 ± 0.5
PLAPP1 2	Co-continuous morphology	–	2039 ± 70	18	19 ± 3	24	3.3 ± 0.23
PLAPP1 S	22	1.4	2525 ± 26	38	48 ± 4	35	15 ± 2
PLAPP2 A	8.9	1.2	2240 ± 64	30	53 ± 7	28	13 ± 2
PLAPP2 B	5.8	1.5	2250 ± 57	27	113 ± 15	39	33 ± 4
PLAPP2 C	8.1	1.1	1996 ± 103	35	77 ± 10	29	15 ± 2
nPLA	–	–	3636 ± 108	–	1.8 ± 0.1	55	0.62 ± 0.04
nPLAPP1 1	4.4	1.4	2404 ± 10	28	10 ± 2	27	2.3 ± 0.2
nPLAPP1 2	Co-continuous morphology	–	2297 ± 15	22	–	21	–
nPLAPP1 S	–	–	2713 ± 98	36	15 ± 2	34	4.7 ± 0.5
nPLAPP2 A	3.4	1.1	3123 ± 64	32	13 ± 2	45	5.6 ± 0.5
nPLAPP2 B	13	1.5	2459 ± 58	28	19 ± 3	33	6.2 ± 0.6
nPLAPP2 C	–	–	2641 ± 98	47	12 ± 3	31	3.8 ± 0.5

Young's modulus (E), yield stress (σ_y), tensile strength (σ_b), elongation at break (ε_b), and tensile toughness (EF)

The isothermal degradation of the neat PLA presented before (Figs. 2, 3) was made in the dynamic rheometer under isothermal conditions at low frequencies. Nevertheless, the PLA thermo-mechanical degradation in the extruder must be different because the processing conditions are non-isothermal and very different shear rates can be found in each element of the screw configuration. Therefore, hydrolysis reactions of the PLA matrix could be taken place because of the PLA moisture absorption in the feed hooper of the extruder, although the PLA and its blends and composites were dried before blending. Without thermo-mechanical degradation of PLA in the extrusion process, the viscosity ratio of the blend components (η_{PP1}/η_{PLA}) should be lower than 1 at 200 °C and higher shear rates (kneading elements in the extruder) because of the higher pseudoplastic character of the PP1 dispersed phase than that of PLA. But this viscosity ratio should lower than 1 at high shear rates in the blends with PP2 as dispersed phase. Nonetheless, the reduction of the PLA viscosity by thermo-mechanical degradation and/or hydrolysis reactions in the extruder increases these viscosities ratios along the extruder sections. The influence of processing conditions during melt extrusion on the degradation of poly (lactic acid) has been already investigated [16, 27–31]. This degradation is influenced by the temperature, residence time in the extruder (screw rotation speed and mass flow rate), and the moisture content. Taubner and Shishoo [31] found a reduction in shear viscosity of about 50% at 230 °C and

120 rpm for the samples conditioned at 65% of relative humidity (RH) before measurements.

In polymer blends research, the drop breakup phenomenon has been study extensively but the effect of the degradation (chain scission reactions) of the continuous phase (PLA) during the mixing process has not been fully explored [4, 5, 16]. In the extrusion process, the shear viscosity of PLA (matrix) is reduced and a negative effect on the dispersion of the minority phase (PPs) should be expected. Then, there is an enhancement of the viscosities ratios (η_{PP1}/η_{PLA} and η_{PP2}/η_{PLA}) and a reduction of the matrix shear stress with time. Consequently, an increase of the droplet sizes of the dispersed phase should be obtained. This explains the large sizes of the dispersed phases in the blends without sepiolite clay (Table 6). On the other hand, it has been reported that SEBS-g-MA is an efficient emulsifying agent in PP/PA-6 blends and number-average diameters of the dispersed phases lower that 1 μm have been found in these blends These results have been explained by the emulsifying process where the SEBS-g-MA compatibilizer agent migrates to the melted dispersed phase and a copolymer is formed at the interface that reduces the coalescence of the dispersed phase droplets [4, 5, 32–36]. Nonetheless, in this study, PP1-g-MA seems more efficient than SEBS-g-MA in emulsifying PLAPP1 blends, although one would expect the material with the highest grafting degree to be more reactive toward the PLA (see Table 3). In that sense, the thermal properties of the blend components should have some influence in the morphology of these blends [35].

The mixing of semi-crystalline polymers with different melting temperatures and rheological behavior in extruders is very complex. All the blend components were added together in the first port of the extruder. In the first stage of the extrusion process, the polymer with the lower melting and/or plasticating temperatures forms the continuous phase and in subsequent stages, a phase inversion takes place where the majority phase forms the continuous phase [35]. Since most polymers are immiscible, compatibilizer agents have to be used in blend preparations. It is well known that the compatibilization of immiscible polymer blends could be achieved by adding grafted rubbers that play a role similar to that of emulsifiers in liquid emulsions, as it was said before [4, 5, 32–37]. The PEm-g-MA compatibilizer agent has the lowest melting temperature range from −15 to 90 °C and the SEBS-g-MA is an amorphous material with high plasticating temperatures (180–200 °C). In the TEM micrographs of the PLAPP1 S blend (Fig. 6a), the presence of inclusions in the interior of the large dispersed phase particles can be seen. The OsO_4 agent only stains the polyolefin phase (PP1). These inclusions are considered to be SEBS-g-MA particles trapped within the PP phase like in "salami" morphology because of the differences between the melting and/or plasticating temperatures of the blend components. In the PLAPP1 S blend, the PP melts first (melting range 80–190 °C) with the SEBS-g-MA dispersed in this PP1. When all blend components are melted or plasticated and the phase inversion have taken place, there is a migration of the SEBS-g-MA from both blend components (PLA and PP1) toward the interface and inclusions of SEBS-g-MA in PP1 and presence of this compatibilizer in the interface result.

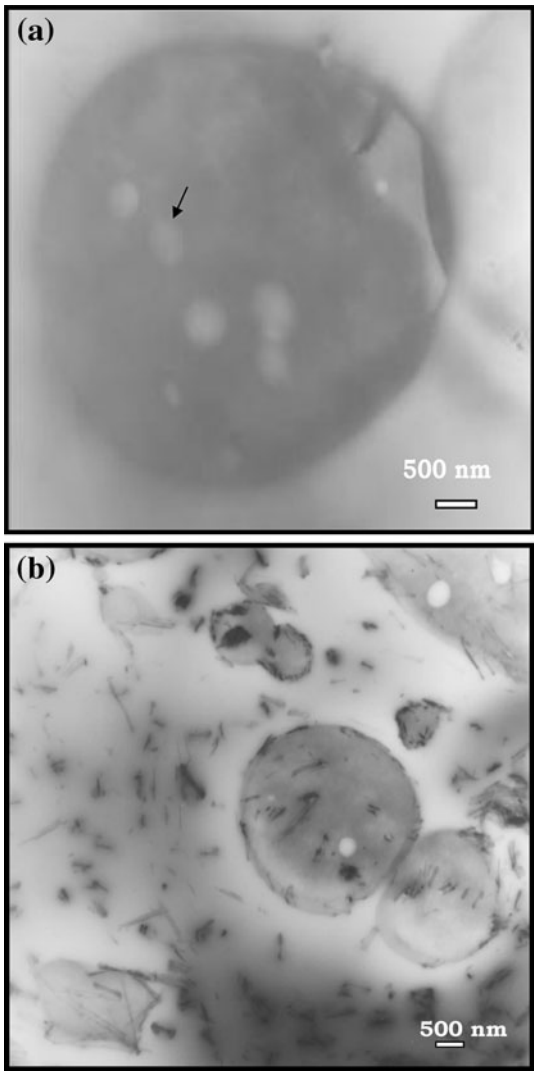

Fig. 6 TEM micrographs of the PLA blend and composite with SEBS-g-MA. **a** Without sepiolite (PLAPP1 S) stained with OsO_4 agent, and **b** with sepiolite (nPLAPP1 S sample) without staining agent

This type of morphology also affects the dispersion of the minor component in PLAPP1 S blend because of its influence on the dispersed phase rheological properties (SEBS-g-MA inside PP1 droplets). Furthermore, there is less amount of SEBS-g-MA available for compatibilization. Then, the efficiency as emulsifying agent of this compatibilizer is reduced. Also, the high concentration of maleic anhydride of the SEBS-g-MA sample in the extruder may induce a higher thermal degradation of the PLA and as a consequence the highest sizes of the dispersed phase in the PLAPP1 S blend (Table 6). However, in the PLAPP1 1, PLAPP2 A, and PLAPP2 C blends, the dispersed phases and the compatibilizer agents melt together (see Tables 2, 5). It is important to point out that the grafting degree of PP1-g-MA, PP3-g-MA, and PEm-g-MA constituting the compatilizer agents is very

similar and lower than that of the SEBS-g-MA sample (Table 3). Thus, the similar particle sizes of the dispersed phase for the PLAPP2 A and PLAPP2 C blends prepared with the same dispersed phase (PP2). The larger droplet sizes of PLAPP1 than those of PLAPP2 A and PLAPP2 C could be ascribed to the higher viscosity ratio of the former. The smallest particle size, in the blends without clay, was found for the PLAPP2 B and the largest one for the PLAPP1 S blend. The PEm-g-MA, used as compatibilizer agent in the PLAPP2 B blend is the component that melts first in the extrusion process (melting range from −15 to 90 °C). When all blend components are melted or plasticated and the phase inversion have taken place, there is a migration of the PEm-g-MA to the PP2 dispersed phase. Thus, the PEm-g-MA material is an efficient emulsifying agent in the PLAPP2 B blend. Nonetheless, small particle sizes of the dispersed phase in this blend without clay could not be obtained because of the enhancement of the components viscosity ratio (η_{PP2}/η_{PLA}) and the reduction of the PLA matrix shear stress along the extruder.

In this research, all the components of the blends were fed through the first port of the extruder and the sepiolite clay (dried before mixing) through the second port. TEM micrographs are shown in Figs. 6b, and 7a, b for the nPLAPP1 S and nPLAPP1 1 in order to analyze the clay dispersion and where it was placed. As can be seen, the morphology of these composites is rather complex because several kinds of particles are shown. These TEM micrographs seem to indicate that the clay resides in the PLA phase and in the PP interface, due probably to the sequence of addition of the components in the extruder and the polar character of the interfaces (SEBS-g-MA and PP1-g-MA). In Figs. 6b and 7a, b single fibrils (about 20 nm of diameter) and some agglomerates of clay with variable dimensions can be seen in both phases (PLA and compatibilizer agent). In both composites (nPLAPP1 S and nPLAPP1 1), the sepiolite clay exhibits nano-dispersed structures with a similar aspect ratio of about 26. In consequence, nPLAPP1 S and nPLAPP1 1 samples could be considered as nanocomposites. In several works [12, 13, 24, 25], the neat polymers with sepiolite were considered to be a nanocomposite because of the excellent distribution of the unmodified inorganic filler in its finest elemental units, even at concentrations as high as 5 wt%, with no indication of particle aggregations. Nonetheless, sepiolite clay agglomerates can be seen in Fig. 7c, d in the nPLAPP2 B composite. The PEm-g-MA (compatibilizer used in this blend) is the material that is first melted in the blending process, as it was said before, and there could be a migration of the sepiolite clay to this melted compatibilizer agent. It was reported that due to the discontinuity of the external silicate sheet, a significant number of silanol groups (SiOH) are present at the whole external surface of the sepiolite [38]. Some particles could be located in this phase because of favorable polymer-particle interactions (hydroxyl groups of the sepiolite and carbonyl groups of the PEm-g-MA compatibilizer agent) [12].

On the other hand, the morphologies of the PLA composites are quite different to that of PLA blends without sepiolite. The smallest particle sizes in the PLA composites were found for the nPLAPP1 C and the largest one for the nPLAPP2 B sample. SEM micrographs of PLA composites (nPLAPP1 1, nPLAPP2 A, nPLAPP2 B, and nPLAPP2 C samples) are presented in Fig. 5. A reduction of the dispersed phase particles can be seen for nPLAPP1 1, nPLAPP1 S, nPLAPP2 A, and

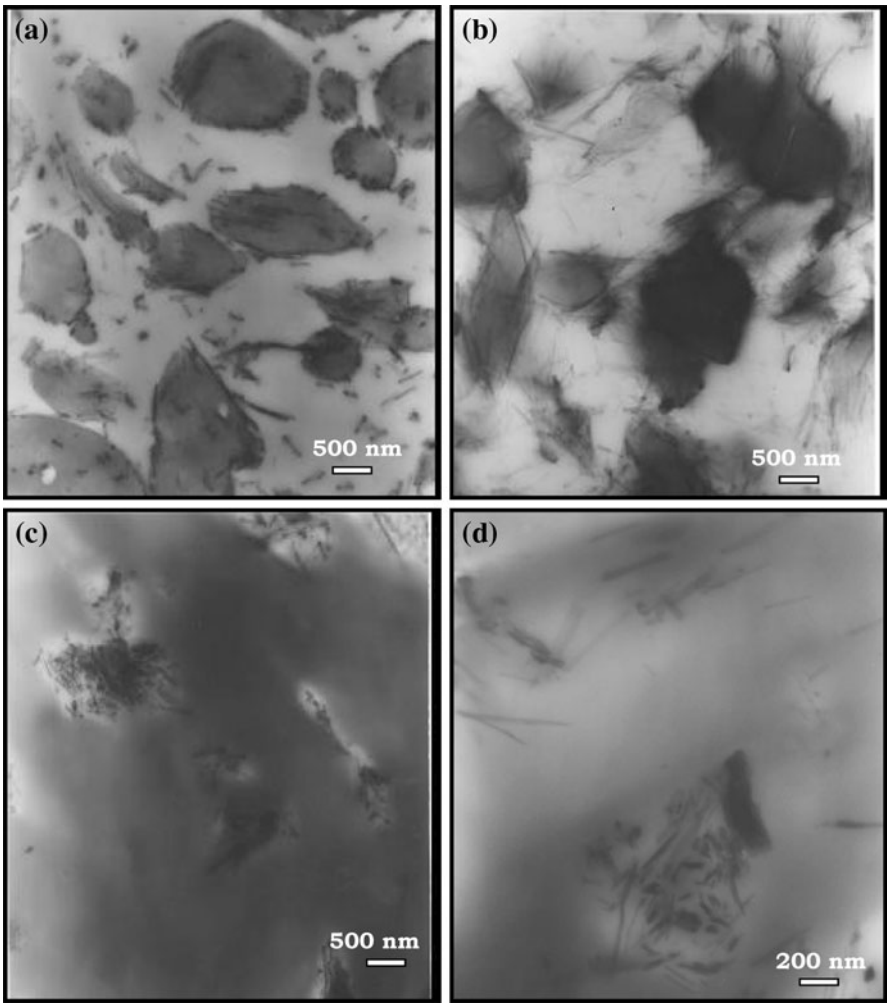

Fig. 7 TEM images of the PLA composites with sepiolite without staining agent. **a** nPLAPP1 S, **b** nPLAPP1 1, **c** nPLAPP2 B, and **d** nPLAPP2 B at higher magnification

nPLAPP2 C composites compared to those in blends without clay (Fig. 5; Table 6). The lower droplet sizes of the dispersed phase for the blends with sepiolite, except for the nPLAPP2 B blend, could be due to the higher viscosity of the PLA nanocomposites and/or higher thermal stability of the nanocomposite at 200 °C (see Table 4). The viscosity ratio of the blend components could be lower than one at high shear rates and a reduction of the sizes of the dispersed phase could be obtained due to the high matrix shear stresses in the extrusion process. Also, the high viscosity of the matrix and the localization of clay at the matrix-dispersed phase interface form a solid barrier that inhibits or prevents the coalescence of the drops [14, 39–41]. Nonetheless, an increase of the dispersed phase particles can be seen for nPLAPP2 B composite compared to those in PLAPP2 B blend without clay

(Table 6; Fig. 7c, d). This result could be due to the migration of the sepiolite clay toward the compatibilizer agent (PEm-g-MA) reducing its emulsifying efficiency and an increase of the dispersed phase particles sizes is obtained. On the other hand, ungrafted monomer (MA) remaining from (or after) the functionalization reactions performed in our laboratory was not completely removed from the grafted materials (PP1-g-MA and PEm-g-MA) used in the mixing procedure, because the grafted products were only washed with acetone. This ungrafted material could promote additional grafting of these samples and/or PLA matrix degradation reactions during the mixing process, which could explain the lower sizes in the nPLAPP2C composite than those of nPLAPP2 A.

Finally, when two immiscible polymers are compounded in mixing equipments, two types of blend morphologies are often observed: dispersed morphology and co-continuous morphology. This last morphology is an unstable intermediate morphology that eventually is transformed into a dispersed morphology at long times for asymmetric blend compositions. This transient co-continuous morphology is influenced by the blend components ratio, thermal properties, rheological behavior, and the processing conditions and equipment employed [35]. A co-continuous morphology was observed for the PLAPP1 2 and nPLAPP1 2 samples (not shown here) because of the high proportion of the PP1 as dispersed phase and the insufficient amount of compatibilizer agent. Hence, a deterioration of the mechanical properties of these blends (Table 6) is obtained.

Tensile properties and rheological behavior of the PLA blends and composites

Table 6 shows the tensile properties, Young's modulus (E), tensile stress at yield (σ_y), tensile strength (σ_b), elongation at break (ε_b), and tensile toughness (the energy consumed during the deformation, EF) of the studied materials. The stress versus elongation curves of the PLA, PP1 and their blends and composites are presented in Fig. 8. Furthermore, the complex viscosity ($\eta^*(0)$), storage modulus ($G'(0)$), and loss modulus ($G''(0)$) at zero time (without degradation effects in the measurement), 200 °C and 0.5 rad/s of frequency are presented in Table 4. The PLA sample is a fragile material with high Young's modulus and tensile strength. In order to balance this behavior, a polyolefinic phase (PP) was incorporated to the PLA. Since PPs added as dispersed phases have lower Young's modulus, tensile strength, and higher viscosity than those of PLA, the blends without sepiolite must also have lower Young's modulus, tensile strength than those of PLA. In addition, all the studied PLA blends and composites display a yield stress, and higher elongation at break and tensile toughness than those of neat PLA and the nanocomposite of PLA (nPLA). The composition of the blends and their morphology, and the properties of the blend components are also important factors to be taken into consideration when discussing their tensile and rheological properties. Moreover, the degree of functionalization and tensile properties of the compatibilizer agent also affect the mechanical behavior as a consequence of the adhesion between the phases and cavitations process [4, 5, 32–37]. Both grafted PPs have higher Young's modulus and tensile strength than the grafted PEm and similar grafting degree (see Table 3).

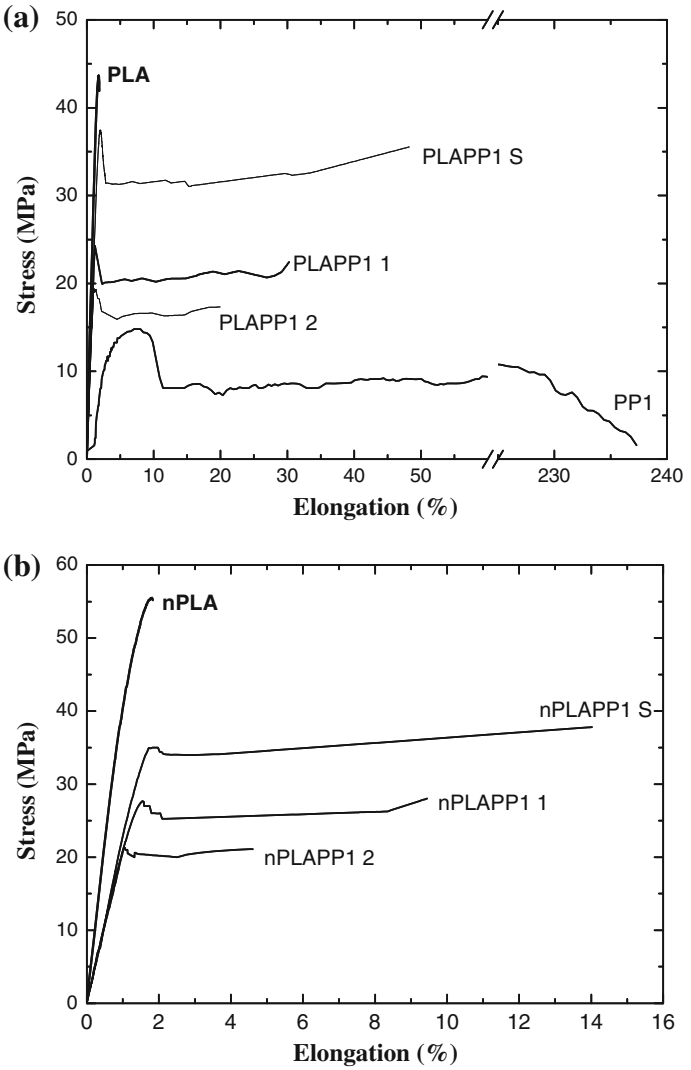

Fig. 8 Stress-elongation curves at room temperature of neat PLA, its blends and composites with PP1 as dispersed phase. **a** neat PLA and its blends and **b** PLA composites

Then, the effectiveness of PP1-g-MA and PP3-g-MA as toughening agents should be lower than that of PEm-g-MA [32, 33, 37].

From the morphology point of view, blends without sepiolite with 17 wt% of PP such as that of PLAPP1 1 have lower tensile strength and toughness, and viscosity and storage modulus values than those of PLAPP2 C sample, prepared with the same compatibilizer agent (PP1-g-MA), due to the larger particle sizes of the dispersed phase in the former. The blend with PP2 as the dispersed phase prepared with PEm-g-MA (PLAPP2 B) has the highest tensile strength and tensile toughness due to its morphology and the tensile properties of the compatibilizer agent employed.

Nevertheless, reductions of 21 and 5% of the tensile modulus and tensile strength, respectively, compared to PLA were obtained. On the other hand, the highest grafting degree of the SEBS-g-MA increases the interactions between the blend components and an increase in the tensile properties could be expected. Nonetheless, the large particle sizes of the dispersed phase in the PLAPP1 S blend (see Table 6) and the degradation of the PLA matrix reduced the effect of these interactions and lower viscosity and storage modulus than those of PLAPP1 1 blend were found.

In that concern, the blends prepared with the PP2 as dispersed phase, and PP1-g-MA and PP3-g-MA as compatibilizer agents (PLAPP2 A and PLAPP2 C blends) have similar elongation at break and complex viscosity, but lower tensile strength, Young's modulus, storage modulus, tensile toughness, and particle sizes of the dispersed phase were obtained for the PLAPP2 C blend. The ungrafted maleic anhydride in PP1-g-MA and PEm-g-MA could promote additional grafting of these materials and/or PLA matrix degradation reactions during the mixing process, as it was said before. Hence, additional grafting obtained during mixing of these materials and as a consequence higher interactions between the blend components may be obtained in the blends prepared with these compatibilizer agents. However, a reduction in viscosity and storage modulus values should be found because of the degradation of the PLA matrix. A balance of these processes determined the tensile and rheological properties in these blends. Nonetheless, not a significant increase in the elongation at break, tensile toughness, complex viscosity, and storage modulus was found for the blend with a higher content of PP1 (PLAPP1 2 sample) due to its co-continuous morphology.

On the other hand, the change in the value of the Young's modulus and in the tensile strength of the PLA, and in the samples with and without sepiolite is related to the fact that the filler incorporation produces an increase in the stiffness of the material. This phenomenon can be explained considering that the filler, besides being incompressible and undeformable, provides a high contact surface area due to the adequate dispersion in the matrix, promoting an increase in the filler–polymer interactions responsible for the reinforcement level, and the increase in the complex viscosity and melt elasticity [35, 36]. Usually, the uniform dispersion of a montmorillonite layered clay results in increase of the tensile strength and modulus of PLA nanocomposites [9–12, 29, 42, 43]. Although detailed description of the surface chemistry of sepiolite was not known, some interactions between the sepiolite clay and the PLA matrix must exist. These interactions could be originated from the hydrogen bonding between the carbonyl groups of the PLA matrix and the hydroxyl groups of the unmodified sepiolite, where the enhanced melt viscosity and tensile strength of the PLA nanocomposite (nPLA) could be attributed to the flow restrictions of PLA chains caused by these interactions [1, 2, 44, 45]. In the composite materials, the addition of sepiolite into the PLA allows obtaining nucleated PLA with a little higher degree of crystallinity than that of neat PLA (see Table 5) that also increases its Young's modulus. Higher Young's modulus of a polyamide-6 nanocomposite with sepiolite than a similar one with montmorillonite was obtained by Xie et al. [12] and Bilotti et al. [29]. The high tensile strength in the nanocomposite with sepiolite (nPLA) obtained in the present study could also be due to the orientation of the single fibers during the tensile test and/or interactions

between the sepiolite clay and the PLA matrix, as it was said before. The enhancements in storage modulus (E') at 30 °C obtained by Fukushima et al. [13] in PLA nanocomposites prepared with montmorillonite (Cloisite 30 B) and sepiolite were 17 and 25%, respectively. In this study, the increases in tensile strength and modulus of the PLA nanocomposite (nPLA) based on sepiolite prepared by extrusion are 34 and 26%, respectively. Furthermore, not a significant reduction of the elongation at break is found in this material.

In addition, the filler dispersion and concentration and the blend morphology are important factors to be taken into consideration when discussing the final clay reinforcement in the composite blends. Moreover, the degree of functionalization and tensile properties of the compatibilizer agents also affect the mechanical and rheological behavior as a consequence of the adhesion between the phases and/or cavitations process, as it was said before. In this sense, the values of elongation at break, Young's modulus, and yield and tensile stress, and viscosity and storage modulus values of the nPLAPP1 S are higher than those of nPLAPP1 1 composite with similar particle sizes of the dispersed phase (see Fig. 7a, b). The composite blends have a higher Young's modulus, similar yield stress than those of the blends without clay. Nevertheless, the presence of sepiolite in the PP interface and/or in the compatibilizer agents reduces the ability to cavitate and the effectiveness of these compatibilizer agents, resulting in an expected lower elongation at break than those of the blends without clay. However, a higher elongation at break is obtained in these blends than those of neat PLA and the PLA nanocomposite (nPLA). The highest tensile toughness and elongation at break were also found in the PLA composite prepared with PP2 as dispersed phase and PEm-g-MA as compatibilizer agent. But due to the highest particle sizes of the dispersed phase and poor dispersion of the sepiolite clay, a reduction of the tensile strength was obtained. On the contrary, the highest tensile strength and modulus were found for the nPLAPP2 A sample and the lowest in the material with 60/40 composition (nPLAPP1 2 blend), due also to its co-continuous morphology.

Regarding the rheological behavior of the PLA composite blends prepared in this study, higher complex viscosity and storage modulus values at zero time of the PLA composite blends than those of the nPLA and blends without clay were also obtained. The highest viscosity and storage modulus values were found for the nPLAPP1 C nanocomposite blend. However, higher storage modulus than loss modulus values (solid-like behavior) were obtained for the nPLAPP1 S composite blend, that can not be justified by the particle size values of the dispersed phase (see Fig. 7a). This last result could be only explained by interactions originated from the hydrogen bonding between the carbonyl groups of the compatibilizer agents and the hydroxyl groups of the unmodified sepiolite and/or high dispersion of the clay in this composite. A balance of the interactions between the unmodified sepiolite and carbonyl groups of the compatibilizers, the dispersion of the sepiolite clay, the blend morphology, the degradation of the PLA matrix in the mixing process, and the type, content and tensile and rheological properties of blend components determined the tensile and rheological properties in the composite blends studied, respectively.

Conclusions

The effectiveness of the grafted materials employed as tensile toughening agents in the studied blends and composites was confirmed by the presence of a yield peak in the tensile stress curves and the increase of the elongation at break and the energy consumed during the deformation. A reduction of the viscosity and storage modulus values with time was found for the neat PLA and PLA blends without sepiolite because of the thermo-oxidative degradation of the neat PLA and PLA matrices of the blends in the dynamic rheometer at 200 °C. However, a lower variation of the viscosity with time was found for the PLA blends than that of neat PLA due probably to the presence of the PPs phases with a higher thermal stability. The large sizes of the dispersed phases in the PLA blends without clay could be attributed to the thermal degradation of the PLA matrix during the extrusion process. Results showed that the compatibilized blends prepared without clay have higher isothermal degradation susceptibility and tensile toughness than those prepared with sepiolite. The presence of sepiolite in the PP interface and/or in the compatibilizer agents reduces the ability to cavitate and the effectiveness of these compatibilizer agents, resulting in lower elongation at break than those of the blends without clay. Nonetheless, the nanocomposite blends exhibited lower tensile strength and Young's modulus values and an increase in elongation at break, tensile toughness, complex viscosity, and storage modulus compared to those of the nanocomposite of PLA (nPLA). The composite prepared with PEm-g-MA and PP2 as the dispersed phase (PLAPP2 B) was the toughest one.

Acknowledgments The authors thank the financial support from Simón Bolívar University (Grupo G-014), the Ministerio de Educación y Ciencia/Spain (MAT2008-06379) and the Junta de Castilla y León (GR104). The authors also thank Propilven C. A. for supplying the PP.

References

1. Sinha Ray S, Okamoto M (2003) Polymer/layered silicate nanocomposites: a review from preparation to processing. Prog Polym Sci 28:1539
2. Pavlidov S, Papaspyrides CD (2008) A review on polymer-layered silicate nanocomposites. Prog Polym Sci 33:1119
3. Garlotta D (2001) A literature review of poly(lactic acid). J Polym Environ 9:63
4. Paul DR, Newman S (1978) Polymer blends. Academic Press, New York
5. Baker W, Scott C, Hu G-H (2001) Reactive polymer blending. Hanser Publisher, Cincinnati
6. Wang Y, Hillmyer MA (2001) Polyethhylene-poly(L-lactide) diblock copolymers: synthesis and compatibilization of poly(L-lactide)/polyethylene blends. J Polym Sci Polym Chem 39:2755
7. Reddy N, Nama D, Yang Y (2008) Polylactic acid/polypropylene polyblend fibers for better resistance to degradation. Polym Degrad Stab 93:233
8. Chang-Hong H, Wang C, Lin C, Lee Y (2008) Synthesis and characterization of TPO–PLA copolymer and its behaviour as compatibilizer for PLA/TPO blends. Polymer 49:3902
9. Bourbigot S, Fontaine G (2008) Processing and nanodispersion: a quantitative approach for polylactide nanocomposite. Polym Test 27:2
10. Sinha Ray S, Maiti P, Okamoto M, Yamada K, Ueda K (2002) New polylactide/layered silicate nanocomposites. 1. Preparation, characterization and properties. Macromolecules 35:3104
11. Sinha Ray S, Bousmina M (2005) Biodegradable polymers and their layered silicate nanocomposites: in greening the 21st century materials world. Prog Mater Sci 50:962

12. Shaobo X, Zhang S, Wang F, Yang M, Séguéla R, Lefebvre JM (2007) Preparation, structure and thermomechanical properties of Nylon-6 nanocomposites with lamella-type and fiber-type sepiolite. Comp Sci Technol 67:2334
13. Fukushima K, Tabuani D, Camino G (2009) Nanocomposites of PLA and PCL based on montmorillonite and sepiolite. Mater Sci Eng 29:1433
14. Fenouillot F, Cassagnau P, Majesté JC (2009) Uneven distribution of nanoparticles in inmiscible fluids: morphology development in polymer blends. Polymer 50:1333
15. Helmy AK, de Busetti SG (2008) The superface properties of sepiolite. Appl Surf Sci 255:2920
16. Signori F, Coltelli M, Bronco S (2009) Thermal degradation of poly(lactid acid) (PLA) and poly(butylene adipate-co-terephthalate) (PBAT) and their blens upon melt processing. Polym Degrad Stab 94:74
17. Han DC (2007) Rheology and processing of polymeric materials. Polymer rheology, vol 1. Oxford University Press, Oxford
18. Minoshima W, White JL, Spruiell JE (1980) Experimental investigation of the influence of molecular weight distribution on the rheological properties of polypropylene melts. Polym Eng Sci 20:1166
19. Nachtigall SMB, Baumhardt Neto R, Mauler RS (1999) A factorial design applied to polypropylene functionalization with maleic anhydride. Polym Eng Sci 39:630
20. Moad G (1999) Synthesis of poluolefin graft copolymers by reactive extrusion. Prog Polym Sci 24:81
21. Kim ES, Kim BC, Kim SH (2004) Structural effect of linear and star-shaped poly(L-lactic acid) on physical properties. J Polym Sci Polym Phys 42:939
22. Wunderlich B (1990) Thermal analysis. Academic Press, London
23. Benavente R, Pérez E, Quijada R (2001) Effect of comonomer content on the mechanical parameters and microhardness values in poly(ethylene-co-1-octadecene) synthesized by a metallocene catalyst. J Polym Sci Polym Phys 39:277
24. Hapuarachchi TD, Peijs T (2010) Multiwalled carbon nanotubes and sepiolite nanoclays as flame retardants for polylactide and its fibre reinforced composites. Composites 41:954
25. Tartaglione G, Tabuani D, Camino G, Moisio M (2008) PP and PBT composites filled with sepiolite: morphology and thermal behaviour. Comp Sci Tech 68:451
26. Varela C, Rosales C, Perera R, Matos M, Poirier T, Blunda J (2006) Functionalized polypropylenes in the compatibilization and dispersion of clay nanocomposites. Polym Compos 27:451
27. Liu X, Zou Y, Li W, Cao G, Chen W (2006) Kinetic of thermo-oxidative and thermooxidative and thermal degradation of poly(d,l-lactide) (PDLLA) at processing temperature. Polym Degrad Stab 91:3259
28. Zhou Q, Xanthos M (2009) Nanosize and microsize clay effects on the kinetic of the thermal degradation of polylactides. Polym Degrad Stab 94:327–338
29. Bilotti E, Zhang R, Deng H, Quero F, Fischer HR, Peijs T (2009) Sepiolite needle-like clay for PA6 nanocomposites: an alternative to layered silicates? Comp Sci Tech 69(15–16):2587
30. Pillin I, Monrelay N, Bourmaud A, Grohems Y (2008) Effect of thermo-mechanical cycles on physico-chemical properties of poly(lactic acid). Polym Degrad Stab 93:321
31. Taubner V, Shishoo R (2001) Influence of processing parameters on degradation of poly(L-lactide) during extrusion. J Appl Polym Sci 79:2128
32. Kim GM, Michler GH, Rösch J, Mülhaupt R (1998) Micromechanical deformation processes in thoughened PP/PA/SEBS-g-MA blends prepared by reactive processing. Acta Polym 49:88
33. Wilkinson AN, Clemens ML, Harding VM (2004) The effect of SEBS-g-maleic anhydride reaction on the morphology and properties of polypropylene/PA6/SEBS ternary blends. Polymer 45:5239
34. Kusmono, Mohd Ishak ZA, Chow WS, Takeichi T, Rochmadi (2008) Compatibilizing effect of SEBS-g-MA on the mechanical properties of different types of OMMT filled poluamide 6/polypropylene nanocomposites. Composites 39:1802
35. Han CD (2007) Rheology and processing of polymeric materials, polymer processing, vol 2. Oxford University Press, Oxford
36. Rosales C, Contreras V, Matos M, Perera, Villarreal N, García-López D, Pastor JM (2008) Morphological, rheological and mechanical characterization of polypropylene nanocomposite blends. Nanosci Nanotechnol J 8:1762
37. Bai SL, G′Sell C, Hiver JM, Mathieu C (2005) Polypropylene/polyamide 6/polyethylene-octene elastomer blends. Part 3. Mechanisms of volume dilatation during plastic deformation under uniaxial tension. Polymer 46:6437
38. Grim R (1962) Clay mineralogy. McGraw-Hill, New York

39. Chow WS, Bakar AA, Mohd ZA, Karger-Kocsis J, Ishiaku US (2005) Effect of maleic anhydride-grafted ethylene–propylene rubber on the mechanical, rheological and morphological properties of organoclay reinforced polyamide6/polypropylene nanocomposites. Eur Polym J 41:687
40. Gallego R, García-López D, López-Quintana S, Gobernado-Mitre I, Merino JC, Pastor JM (2008) Influence of blending sequence on micro- and macrostructure of PA6/mEPDM/EPDMgMA blends reinforced with organoclay. J Appl Polym Sci 109:1556
41. Dasari A, Yu ZZ, Mai YW (2005) Effect of blending sequence on microstructure of ternary nanocomposites. Polymer 46:5986
42. Sinha Ray S, Yamada K, Okamoto M, Ueda K (2003) New polylactide-layered silicate nanocomposites. 2. Concurrent improvements of material properties, biodegradability and melt rheology. Polymer 44:857
43. Arroyo OH, Huneault MA, Favis BD, Bureau MN (2010) Processing and properties of PLA/thermoplastic starch/montmorillonite nanocomposites. Polym Compos 31:114
44. Galgali G, Ramesh C, Lele A (2001) A rheological study on the kinetics of hybrid formation in polypropylene nanocomposites. Macromolecules 34:852
45. Durmus A, Kasgoz A, Macosko CW (2007) Linear low density polyethylene (LLDPE)/clay nanocomposites. Part I: Structural characterization and quantifying clay dispersion by melt rheology. Polymer 48:4492